SAE INTERNATIONAL

ARTICLE INFO
Article ID: 10-10-02-0010

doi:10.4271/10-10-02-0010

Measurement of Light Truck Tire Operating Deflection Shapes Using Scanning Doppler Laser Vibrometry: Issues and Insights

Jennifer M. Bastiaan,[1] Gaurav Chauda,[2] Javad Baqersad,[1] Arjun Gupta,[1] and Kevalya Dhami[1]

[1]*Kettering University, Mechanical Engineering. USA*
[2]*Yokohama Tire, USA*

Abstract

As internal combustion engines are replaced by quieter electric motors in ground vehicles, noise and vibration sources aside from the powertrain have become relatively more important. This is especially true of tires. Measurement of the dynamic vibratory characteristics of tires is critical to understanding their influence on the noise and vibration performance of vehicles, both outside the vehicle body and inside of it. In this work, the normal modes and operating deflection shapes of a Yokohama Geolander A/T light truck tire are measured using traditional modal analysis techniques as well as a non-contact Scanning Laser Doppler Vibrometry (SLDV) approach. Boundary conditions including free, fixed, loaded, and rotating are implemented to the tire and investigated. Rotating conditions are accomplished in a physical chassis dynamometer environment, with the measured tire mounted on the front axle of a Chevrolet Silverado 1500 pickup truck. Modes of vibration and associated natural frequencies that are measured in all four boundary conditions, including steady-state rotation, are reported and illustrated. Results of the study show that operating deflection shapes of a rotating light truck tire can be measured on a chassis dynamometer using SLDV, assuming the tire is undergoing steady-state rotation, but certain disadvantages in the dynamometer environment make the measurement procedure challenging. Specific concerns such as tire rotating speed consistency and sufficient spatial and frequency resolution of the measurements are delineated in this work. Moreover, practical recommendations for measurement of rotating tire operating deflection shapes using a SLDV are included, and a comparison with the Digital Image Correlation (DIC) method of measurement is presented.

History

Received: 20 Jun 2025
Revised: 04 Nov 2025
Accepted: 15 Dec 2025
e-Available: 10 Feb 2026

Keywords

Tire Vibration, Scanning Laser Doppler Vibrometry, Operating Deflection Shapes, Modal Analysis, Tire Natural Frequencies, Tire Damping

Citation

Bastiaan, J., Chauda, G., Baqersad, J., Gupta, A. et al., "Measurement of Light Truck Tire Operating Deflection Shapes Using Scanning Doppler Laser Vibrometry: Issues and Insights," *SAE Int. J. Veh. Dyn., Stab., and NVH* 10(2):211-235, 2026, doi:10.4271/10-10-02-0010.

ISSN: 2380-2162
e-ISSN: 2380-2170

1. Introduction

Tires have always had an important influence on the sound and vibration behavior of ground vehicles, and this is especially true in the new era of electrification. Electric vehicles are increasing in popularity with consumers due to high fuel prices and environmental concerns [1]. Nevertheless, electric vehicles are significantly quieter than the traditional vehicles with internal combustion engines that they are replacing. Of the four main sources of pass-by noise in a traditional vehicle, the: (1) internal combustion engine, (2) air induction system, (3) exhaust system, and (4) tires, only the tires carry over as a noise source into electric vehicles [2]. Furthermore, the contribution of tire noise remains significant for all vehicles, regardless of propulsion type [3].

Fundamental to characterizing the dynamic behavior and response of tires is the use of modal analysis testing [4]. Conventional modal analysis test methods involve instrumented impact hammers or electrodynamic shakers, as well as accelerometers or strain gauges for vibration measurement. These modal analysis tools have been used successfully with tires, especially when the tire is not rotating [5]. However, conventional tools become difficult to use when a tire under test is rotating. In this study, an investigation of the use of non-contact methods for measuring tire vibration during modal analysis testing is performed. The modes of a light truck tire are physically determined using a Scanning Laser Doppler Vibrometry (SLDV) vibration measurement system, in both non-rotating and rotating conditions. The objective of the study is to determine if SLDV can be used to measure the operating modes of a tire, and if so, what are the practical limitations and challenges of using a SLDV system. The key scientific contributions of this work are enumerated as follows:

1. ***Enhanced understanding of tire modes of vibration under rotation.*** New insights into the dynamic behavior and mode shapes of rotating tires are supplied, expanding the current knowledge in this area.
2. ***Effect of boundary conditions on tire modes of vibration.*** The influence of boundary conditions on tire modal characteristics is demonstrated, including when the tire is rotating, which has not been thoroughly analyzed in prior work.
3. ***Comprehensive comparative summary of tire vibration measurement methods.*** A conclusive table is provided that summarizes findings from various measurement technologies including contact sensors, Digital Image Correlation (DIC), and SLDV. This table serves as a practical guideline for engineers and researchers to understand the strengths and limitations of each technique when applied to tire dynamics.

2. Literature Review

Vibration of tires has traditionally been measured using accelerometers and strain gauges. Such modal measurements are typically conducted under laboratory conditions, where tires are tested in either free or fixed boundary states and are excited using mechanical shakers or modal impact hammers [6–9]. However, applying conventional accelerometer and strain gauge–based methods to rotating tires poses significant challenges, primarily due to wiring constraints and data transmission issues. While researchers have attempted to adapt accelerometers and strain gauges for rotating tire measurements, with some employing wireless accelerometers and wireless data acquisition systems [10, 11], practical difficulties persist.

To address these limitations, non-contact optical methods have become increasingly popular for measuring vibrations in rotating structures [12]. Among these, DIC [13] and SLDV [14] are commonly used. Optical methods offer key advantages, most notably the elimination of physical wiring or direct data transmission connections, making them ideal for measuring vibrations in rotating systems. Broadly, these optical methods can be categorized into two groups: (1) white light–based methods (e.g., DIC and computer vision) and (2) laser-based methods [e.g., Laser Doppler Vibrometry (LDV)]. White light–based methods, such as DIC, employ the principles of photogrammetry to measure structural displacements [13]. In three-dimensional DIC, two cameras capture images simultaneously, and the 3D coordinates of points on the structure are determined using a stereo-triangulation approach [15]. DIC was first introduced by Peters and Ranson in 1980 [16] and significantly developed by Chu and Sutton [17, 18], originally for measuring deformations in solid mechanics and quasi-static phenomena [19]. The technique works by tracking subsets of a speckled pattern across sequential images to determine displacement fields [20].

With advances in high-speed imaging, DIC has been extended to dynamic applications and transient phenomena. It has been successfully employed to measure vibrations in diverse systems, including bridges [21], musical instruments [22], civil infrastructures [23], full-size vehicles [24], human skin [25], and bolted joints [26]. Researchers have further adapted DIC to vibration measurements in rotating contexts, such as wind turbine blades [27], helicopter rotors [28], and tires [29–32]. Despite its broad applicability, DIC can be limited by relatively long data processing times [33], the risk of aliasing, and susceptibility to harmonic noise.

LDV was developed in the 1960s to measure fluid velocities [34] and was later adapted for vibration measurements [35–37]. By exploiting the Doppler effect, an LDV system enables non-contact velocity measurements of a target surface [38]. LDV offers full-field,

non-intrusive measurements that circumvent many limitations of contact-based methods. In SLDV, a scanning mirror directs a laser beam across the test surface to obtain measurements over a broad field. A single laser vibrometer measures only out-of-plane displacements, so acquiring three-dimensional vibration data requires a system of three lasers [39]. SLDV is especially useful for vibration analysis due to its high precision and capacity to capture high-frequency vibrations without any physical attachment to a structure. LDV has been extensively used to investigate the vibrations of diverse structures, including bridges [40], non-rotating turbine blades [41], hard disk drives [42], biomedical components [43], and non-rotating tires [44]. Additionally, it has been used in structural health monitoring environments [45]. However, its application to rotating structures presents unique challenges. SLDV measurements on rotating bodies can be carried out in two main ways: (1) a Lagrangian (tracking) approach, in which the laser tracks a specific point moving with the rotating object, or (2) an Eulerian (stationary) approach, where the laser remains fixed in space while the object rotates past the measurement point [46].

The Lagrangian approach has been used to measure vibrations in small sections of rotating tires, timing belts [46], and rotating blades [47, 48]. One way to facilitate measurements in the Lagrangian frame is to employ a derotator or rotate the laser itself [49]. Conversely, the Eulerian approach measures deformations as they pass through the fixed laser spot, effectively capturing "stationary" data of the rotating structure's vibration profile over time. In the present study, a SLDV system is used to measure vibrations on a rotating tire using an Eulerian approach. SLDV measurements are made on a rotating tire, and a detailed procedure for data acquisition is provided. The work is intended to show how the tire resonant frequencies change in different boundary conditions including free, fixed, loaded, and rotating. Furthermore, a comparative discussion on the advantages and disadvantages of SLDV, DIC, and traditional pointwise sensor vibration measurement methods is supplied in a summary table, highlighting considerations such as measurement resolution, setup complexity, and applicability to various test scenarios.

3. Vehicle, Tire, and Test Setup

A light truck tire was tested on a pickup truck in a chassis dynamometer environment. The tire was a Yokohama Geolander A/T 275/60 R 20 115H. The test vehicle was a 2022 Chevrolet Silverado 1500, as shown in Figure 1. The vehicle condition shown is as installed in the test cell, which was equipped with a Super Flow AutoDyn All Wheel Drive chassis dynamometer. The Silverado was restrained with cinch tie-down straps made from polyester with heavy-duty stitching. The Geolander tires were installed at all four corners of the Silverado test vehicle, with vehicle manufacturer torque specifications applied to the lug nuts. Once the vehicle was inside the test cell, only the right front tire was measured. Data were collected at a vehicle speed of 30 MPH (48 KPH), which is a typical driving speed on city streets. At 30 MPH, the fundamental rotational frequency of the spinning right front tire was 5.1 Hz. The Geolander tires, which were mounted on aftermarket wheels and balanced prior to dynamometer testing, were also investigated in a laboratory setting as stand-alone components without installation on the vehicle. Laboratory testing was used for non-rotating modal analysis procedures, whereas the chassis dynamometer environment was employed to perform both non-rotating modal analysis and Operating Deflection Shape (ODS) testing of the rotating right front tire.

FIGURE 1 2022 Chevrolet Silverado 1500 test vehicle.

3.1. Boundary Conditions

Boundary conditions for the tire testing in both laboratory and dynamometer environments are summarized in Table 1. The right front tire was measured during loaded testing on the chassis dynamometer, as highlighted in Table 1. In this condition, the vehicle was parked in the dynamometer cell, and the tire was measured using the SLDV non-contact measurement method; the wheels were not rotating. The load applied to the right front tire was 6116 N. Note that this was about 19% higher than the vertical load of 5158 N applied in the (tire-only) laboratory environment, where conventional contact measurement methods were used. The lower load represents the corner load on each of the rear wheels. When the laboratory testing was being performed early in the project, it was expected that one of the rear tires would be tested on the chassis dynamometer. Once onsite at the dynamometer, however, the logistics of the measurement setup

TABLE 1 Boundary conditions used in tire testing.

Boundary condition	Short description	Test setup	Test environment
Free–free	Free	Wheel/tire was suspended from bungee cords that were connected to the wheel. No rotation.	(1) Laboratory with conventional and (2) laboratory with non-contact measurement methods.
Fixed	Fixed	Wheel/tire was fixed at the wheel center. No rotation.	(1) Laboratory with conventional and (2) laboratory with non-contact measurement methods.
Fixed and loaded	Loaded	Wheel/tire was fixed at the wheel center and loaded with the vehicle corner weight. Footprint contact existed at the "road" surface. No rotation. Right front tire tested on the dynamometer.	(1) Laboratory with conventional and (2) dynamometer with non-contact measurement methods. Laboratory test had 5158 N vertical load; dynamometer test had 6116 N vertical load.
Fixed, loaded, and rotating	Rotating	Same as fixed and loaded, except the wheel/tire was rotating.	Dynamometer with non-contact measurement methods. Vertical load = 6116 N. Vehicle speed = 30 MPH.

precluded testing of the rear tires. The right front tire was selected for testing instead.

In general, the vertical static stiffness of a light truck tire should not change much with an increase of vertical load from 5158 N to 6116 N. It is possible that there may be a small increase in vertical static stiffness, although this would not likely exceed a few percent [50]. As the tire as a dynamic system was under test in this study, the unchanged tire mass in concert with small modifications to tire static stiffness (from corner load changes) were not expected to alter the modal analysis results significantly. This means that the measured tire natural frequencies should be comparable between the loaded dynamometer test with the higher corner load, and the loaded laboratory test with the lower corner load.

3.2. Data Acquisition

A measurement frequency range of 0–400 Hz was used for SLDV testing in this study, as it should capture the most significant vibratory behavior of a tire, which is determined by its most important normal modes. In general, tire modes with frequencies up to 250 Hz have the largest influence on the overall response of a tire [51]. Above 250 Hz, the normal modes of a tire are usually highly damped and therefore relatively less important. Thus, the 0–400 Hz measurement frequency range was selected to capture the expected primary tire behavior with less damping below 250 Hz, and to confirm the secondary tire behavior with substantial damping above this frequency and up to 400 Hz. In this study, "damping" refers to the dimensionless damping ratio, or fraction of critical damping. Modal curve fitting was used to find damping in most cases. Curve fitting is a method that is employed to extract basic modal parameters from measured data, including frequency, damping, and mode shapes [52]. It can be used to determine damping in closely spaced modes. Whenever curve fitting was not used to find damping, the "three dB down" (i.e., half-power bandwidth) method was used [53].

The SLDV system used in this study employed a digitally implemented Fast Fourier Transform (FFT) algorithm. The frequency range was specified by the instrument operator, along with the number of FFT lines. The frequency resolution of the analysis can be found by dividing the frequency range by the number of FFT lines. The frequency resolution is related to the data acquisition time, with finer resolution requiring more time. In general, the idea is to specify a sufficient number of FFT lines to obtain a desired frequency resolution given a set frequency range. The frequency resolution varied depending on the boundary conditions applied to the tire under test.

4. Conventional Modal Analysis with Accelerometers

Conventional modal testing on the tire was conducted using accelerometers, an instrumented impact hammer, and a shaker. The Siemens Testlab software with a SCADAS-Mobile data acquisition system (48 input channels) was used for data collection. The instruments used in testing and their sensitivities are summarized in Table 2. For the measurement process, accelerometers were attached to the tire using cyanoacrylate superglue. Each test involved 12 tri-axial accelerometers, which were strategically placed across three separate geometrical areas: (1) the front sidewall, (2) the circumferential tread

TABLE 2 Instrumentation details for accelerometers and shaker testing.

Equipment	Specification	Sensitivity
Accelerometers (PCB)	Mounted using superglue	~10 mV/g
Impact Hammer (PCB)	Used for free–free testing	~2.0 mV/N
Integral Shaker (Siemens Qish)	Used for fixed testing	~2.2 mV/N

center, and (3) the back sidewall. During each measurement, all 12 accelerometers were connected to one geometrical area at a time, and the process was repeated for the other two areas.

The roving accelerometer method was used to decrease the total test time to about half an hour. In contrast with the employed strategy of using 12 accelerometers in three different tire regions, a roving impact hammer approach would have consumed more test time, estimated to be between three and four hours. The collected Frequency Response Functions (FRFs) were processed using the Siemens PolyMAX algorithm. The identified mode shapes were analyzed and cataloged along with their corresponding frequencies, allowing for a comprehensive assessment of the tire's dynamic behavior. Three types of tire modal analysis testing were conducted using this process, all in a laboratory setting.

1. **Free Modal Testing:** The tire was suspended using bungee cords attached to the wheel, and an impact hammer excited the tire from three different directions. This setup resulted in the collection of 108 FRFs, obtained from 12 tri-axial accelerometers placed in three different geometrical areas, with impacts applied in three orthogonal directions.
2. **Fixed Modal Testing:** The testing followed a similar approach, but with the tire rigidly mounted on a support at the wheel center, as shown in Figure 2. Instead of an impact hammer, an integral shaker excited the tire at a single point in three different directions, again yielding 108 FRFs. The force applied by the shaker corresponded to excitation at a single reference point where the shaker was attached. During testing, the shaker orientation was changed sequentially to excite the same point in the X-, Y-, and Z-directions, ensuring full directional coverage.
3. **Loaded Modal Testing:** The tire was subjected to a vertical load of 5158 N before conducting the same measurement process as in the fixed test.

FIGURE 2 Fixed testing of the tire using accelerometers and an integral shaker. The tire is fixed at the wheel center in the laboratory. Note the clearance space between the bottom of the tire and the surface below. In the loaded testing, the tire is subjected to a vertical load, and it comes into contact with the surface below.

5. Non-Contact Modal Analysis with SLDV

Non-contact vibration measurements were made using a PSV-500-3D Scanning Vibrometer from Polytec. This is a SLDV measurement system that is designed for non-contact, full-field vibration measurements with high spatial resolution. The system employs three independent laser scanning heads to simultaneously measure in-plane and out-of-plane vibrations. It has a broad measurement frequency range, being capable of measuring mechanical oscillations from 0 to 25 MHz. Two types of tire modal analysis testing were conducted using the SLDV system, with free and fixed boundary conditions, both in a laboratory setting. Two types of tire modal analysis testing were conducted with the SLDV system in a chassis dynamometer environment, one with loaded boundary conditions and the other with a rotating tire that was designed to measure operating modes. For all non-rotating test conditions, an electrodynamic shaker was attached to the tire at a single point. The shaker had an orientation that was oblique with respect to the tire, where the inclination angles were selected to excite as many tire modes as possible. While the shaker attachment point should not influence the extracted modal parameters, it can alter the number of modes measured. In this study, the goal of the shaker setup process was to maximize the number of tire modes excited. In addition, pseudo-random excitation was applied by the shaker.

5.1. Free Modal Analysis

5.1.1. Test Setup In the free boundary condition setup, the tire was suspended using bungee cords attached to

an in-laboratory pulley crane system, as shown in Figure 3. The electrodynamic shaker that was used to excite the tire can be seen in Figure 3. The bungee cord attachment method effectively minimized the stiffness of the external constraints, allowing the tire to oscillate freely in all directions, simulating unconstrained dynamic behavior. To ensure measurement stability and reduce transient oscillations, a settling time was introduced before data acquisition. This pause allowed the system to reach a near-static state, preventing unwanted motion from affecting the results. By allowing the suspended tire to stabilize, the accuracy of the measured vibration response was significantly improved, ensuring high-fidelity data for further analysis.

Throughout the SLDV scanning process, only the lasers were repositioned to capture measurements from different angles (see Figure 4), while the tire remained in its free setup state. This method facilitated a full-field analysis of the tire's tread and sidewall deformations without introducing additional variability due to tire repositioning. The strategic movement of the lasers ensured that comprehensive vibration data was collected across all key structural regions, contributing to a more detailed understanding of the tire's dynamic response.

FIGURE 3 Free testing of the tire using the SLDV system and an electrodynamic shaker. The tire is suspended from bungee cords in the laboratory.

5.1.2. Test Procedure In the free modal analysis test procedure, the tire was divided into four equal sectors, allowing for a structured and systematic scanning process. This segmentation ensured that each section was covered comprehensively while minimizing redundant scans. The reference points for the 3D measurement coordinate system were strategically placed on the edges of the scanning mesh, facilitating accurate alignment between different measurement sectors. By dividing the tire into sectors, the number of scans required to achieve full coverage was reduced, thereby decreasing the overall time required for testing. This approach made the scanning process more efficient while maintaining high-resolution data acquisition for detailed vibration analysis. Measurement sectors in the free modal analysis test are shown in Figure 5. In the free test, the SLDV system operated within a 0–400 Hz frequency range, utilizing 800 FFT lines and three averaging complexes for enhanced signal quality. Each scan point required six seconds to measure, with a total of 1282 scan points and an overall scan duration of 2.13 h.

5.2. Fixed Modal Analysis

5.2.1. Test Setup In the fixed boundary condition setup, the tire was securely mounted on a specially manufactured hub to ensure stability during vibration measurements. The hub was extremely heavy and very low in flexibility, as it was designed to be much more massive and stiff than the wheel and tire assembly under test, for the purpose of minimizing the influence of the hub on the dynamic response of the tire. To further isolate the tire from potential environmental disturbances and maintain consistent boundary conditions, the hub was attached to a massive cast-iron T-slotted bedplate. During the scanning process, only the lasers were repositioned to capture different measurement angles, while the tire itself remained fixed. This approach facilitated a comprehensive full-field analysis of the tire's sidewall

FIGURE 4 Laser perspectives of the tire in free testing using the SLDV system.

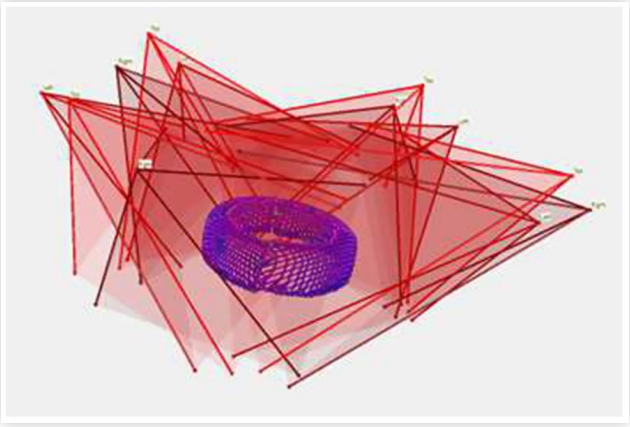

FIGURE 5 Vibration measurement sectors in free testing using the SLDV system.

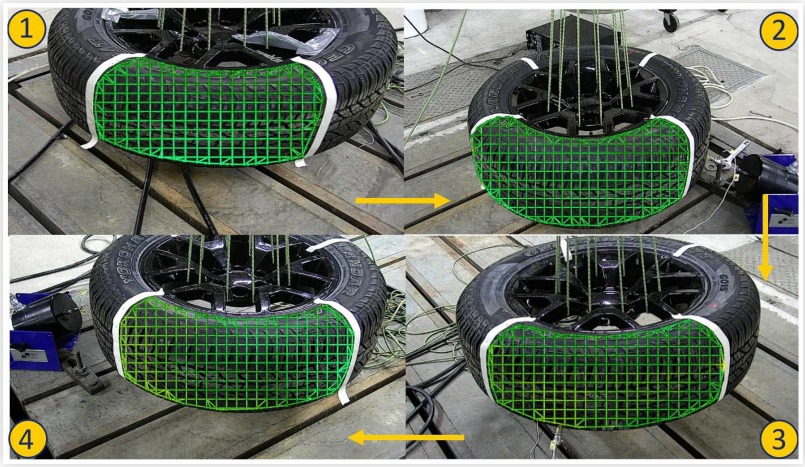

and tread vibration characteristics without introducing additional variability due to tire movement. The laser repositioning strategy provided a multi-perspective dataset essential for capturing the complex deformation behavior of the tire under external excitation from the electrodynamic shaker.

5.2.2. Test Procedure In the fixed modal analysis test procedure, a systematic approach was followed to conduct a comprehensive vibration analysis of the tire. The process began with scanning the sidewall and establishing reference points for subsequent tread scans. These reference points served as critical markers to ensure accurate alignment between multiple scan regions, facilitating the integration of data collected from different measurement perspectives. Once the sidewall reference points were established, the tread was scanned while incorporating these points as 3D spatial coordinates. Measurement regions in the fixed modal analysis test are shown in Figure 6.

Additional reference points were placed on the sidewall, tread, and bedplate to further enhance spatial alignment and ensure precise correlation between different scan sections. This step was repeated systematically until all the tread was fully scanned, ensuring a complete dataset for structural vibration analysis. After data acquisition, the scans were combined and indexed in sequence to maintain the correct spatial mapping of measurement points. In the fixed test, the measurement setup operated within a 0–400 Hz frequency range, utilizing 800 FFT lines and three averaging complexes to enhance the signal-to-noise ratio. The scan time per point was approximately six seconds, with a total of 1610 scan points and an overall scan duration of 2.68 h.

5.3. Loaded Modal Analysis

5.3.1. Test Setup In the loaded tire setup, the test vehicle was secured using harnesses at both the front and rear ends in a chassis dynamometer environment. This approach minimized any unintended vehicle movement that could introduce inaccuracies in the measured vibration data. The immobilization of the vehicle was crucial to isolating the tire's dynamic responses during measurement. Restricting longitudinal vehicle motion allowed for precise tire vibration analysis while mitigating the effect of disturbances from vehicle shunt vibrations. A photograph of the vehicle in the dynamometer environment appears in Figure 7.

Safety protocols of the chassis dynamometer test facility were adopted. The vehicle was tied down to the concrete floor with textile harnesses, which can be seen at the back of the vehicle near the floor in yellow color in Figure 7. The vehicle exhaust was vented to the outside with a flexible exhaust hose, which can be seen in Figure 7 at the back of the vehicle in orange color. A safety driver was inside the vehicle at all times during its operation. The driver kept their hands on the steering wheel during vehicle operation, in case there was an unintended deviation from straight-line driving that needed to be corrected. The driver was also available to activate the brakes in case a situation occurred that required emergency braking. There was a control room adjacent to the dynamometer test cell with large windows, which permitted the test to be visually monitored from outside the cell by engineers on the project team. An emergency stop button was available in the control room to stop the testing if necessary.

To introduce an external excitation source, an electrodynamic shaker was connected to the tire tread with two-part epoxy. This configuration allowed controlled vibrational input to the tire, similar to the forces that were applied in the laboratory testing for the fixed boundary condition case. A photograph of the SLDV system setup in the dynamometer environment appears in Figure 8. From Figure 8, it can be seen that a fourth single-point laser vibrometer was added to the measurement system. This fourth vibration sensor was used as

FIGURE 6 Vibration measurement regions in fixed testing using the SLDV system.

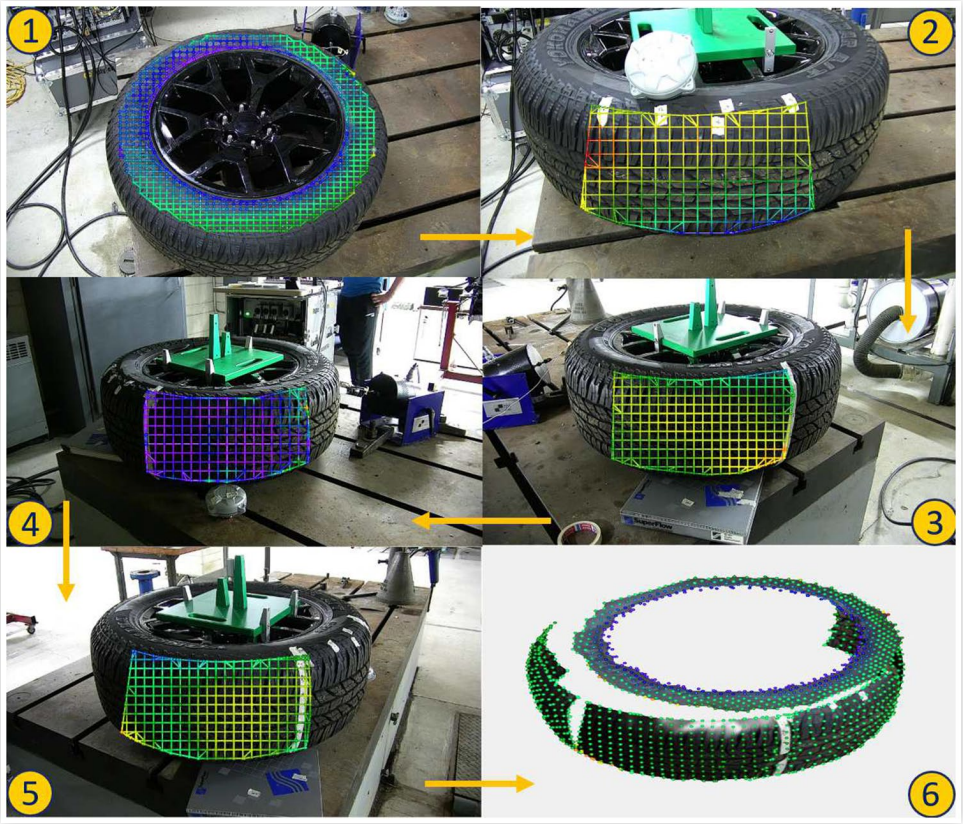

a reference that measured the vibration of the wheel, rather than the tire. The reference measurement was located around 1.5 in (about 4 cm) above the wheel center in a geometrically flat location on the wheel. During the scanning process, all the lasers remained in their original positions and orientations. They were not moved or adjusted as in the laboratory tests. See Figure 9 for a visualization of the measurement angles in the dynamometer environment.

5.3.2. Test Procedure In the loaded modal analysis test procedure, a simplified process was employed to evaluate the vibrational characteristics of the tire sidewall under static loading conditions. The objective was to conduct a focused measurement on the sidewall without including the tread or other components. The procedure involved scanning the sidewall, ensuring a streamlined and efficient data collection process. The method facilitated precise measurement of sidewall deformations and vibrational behavior under parked conditions of the vehicle. In the loaded test, the measurement setup operated within a 0–400 Hz frequency range, employing 1600 FFT lines and five averaging complexes to improve signal clarity. The scan time per point was approximately 20 seconds, with a total of 191 scan points, leading to an overall scan duration of 1.06 hours. This efficient measurement setup provided high-fidelity data for tire sidewall modal analysis.

5.4. Rotating Operating Analysis

5.4.1. Test Setup In the rotating tire setup, the test vehicle was securely fastened using harnesses at both the front and rear ends to maintain stability during testing. This ensured that any recorded vibrations were solely due to the tire's operating conditions and not influenced by unintended vehicle movement. Stabilizing the vehicle was critical to isolating the tire's structural response and obtaining accurate vibration data. To simulate actual operating conditions, a headwind fan was introduced to generate airflow corresponding to vehicle speed. This additional factor helped replicate aerodynamic forces and cooling flows experienced by the tires in motion, providing a more comprehensive simulation of straight-line driving conditions.

5.4.2. Test Procedure In the rotating test procedure, the sidewall was measured using the SLDV system to capture its vibration response under operating conditions. The primary objective was to capture the dynamic behavior of the tire sidewall during simulated vehicle motion. To ensure high-accuracy data acquisition, multiple reference points were incorporated into the

FIGURE 7 Light truck test vehicle in the chassis dynamometer environment.

measurement setup. These references enabled precise synchronization of the vibration data with the overall vehicle dynamics behavior. The reference points included:

1. A tri-axial accelerometer mounted on the right front suspension upright to measure localized chassis vibrations.
2. A tri-axial accelerometer positioned on the outside of the front bumper at the far right, capturing front-end structural responses.
3. A Hottinger Brüel & Kjær Type 2981 laser tachometer mounted on a tripod that was used to measure the angular velocity of the wheel, regulated by retroreflective tape that resulted in a once per wheel revolution signal.
4. A Polytec QTec single-point laser vibrometer mounted on a tripod to measure vibration near the wheel center, serving as a reference for tire motion tracking.

FIGURE 8 SLDV measurement setup in the chassis dynamometer environment for the loaded testing.

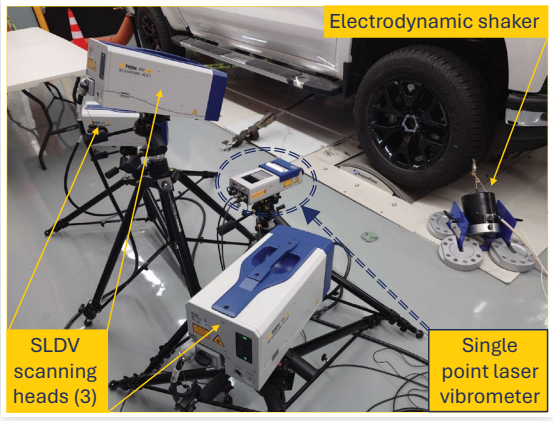

In the rotating test the measurement setup operated within a 0–400 Hz frequency range, employing 200 FFT lines and eight averaging complexes to improve signal clarity. The scan time per point was approximately four seconds, with a total of 329 scan points, leading to an overall scan duration of 0.365 hours. A photograph showing the instrumentation setup for the rotating measurements is shown in Figure 10. All the optical instruments shown had a direct line of sight to the right front tire and wheel of the test vehicle, without any obstructions. A screenshot from the SLDV setup software from the dynamometer environment appears in Figure 11. The measurement points are highlighted in gray color and superimposed onto a photograph of the rotating tire that was made by the SLDV system.

Fewer FFT lines were used in the rotating tire test compared to the tests of non-rotating boundary conditions. Considering the 0–400 Hz frequency range used and the 200 FFT lines specified, this measurement setup resulted in a frequency resolution of 2 Hz. This seemingly rough frequency resolution was recommended by Polytec for rotating tire testing. The idea was to mitigate any inconsistencies in tire rotating speed variation by "averaging" the variation in measured responses, with the objective of bringing the various measurements into single peaks in the resulting frequency spectra. The use of the 2 Hz frequency resolution was also intended to shorten the total testing time on the chassis dynamometer. However, it was primarily implemented to improve the tire mode identification results in the rotating boundary conditions case.

6. Results

This study successfully employed the SLDV technique to capture and analyze the vibrational behavior of a tire under four distinct test conditions: (1) free, (2) fixed, (3) loaded, and (4) rotating. Across all setups, key vibrational modes were identified, showcasing how boundary conditions, static load, and rotating speed influence the modal characteristics and deformation patterns of the tire. The free and fixed tests revealed fundamental structural modes in the unloaded state. The loaded test showed stiffer and more damped responses due to real-world vehicle weight. The rotating tests, conducted at various speeds, captured real-time operating behavior, highlighting rotating speed-dependent mode shifts and resonance phenomena critical to noise and vibration analysis. Overall, the study demonstrates that SLDV provides high-resolution, full-field vibration data, enabling a deeper understanding of tire dynamics.

6.1. Free Modes

Mode shapes and associated natural frequencies for the tire with free boundary conditions are listed in Table 3.

FIGURE 9 Laser perspectives of the tire in loaded testing using the SLDV system. Measurement angles were the same for the loaded and rotating testing.

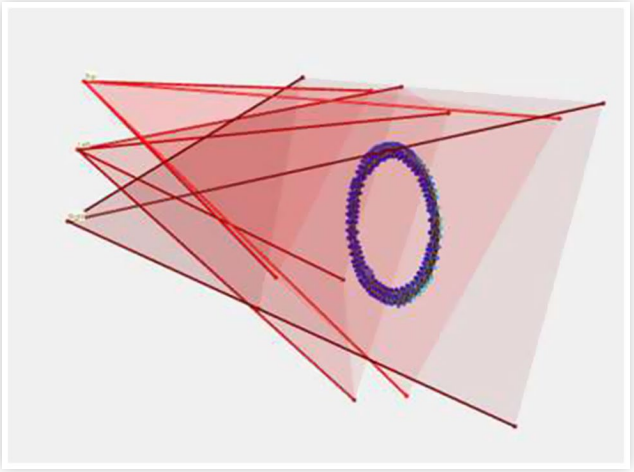

Table 3 provides mode shape descriptions with a numbering scheme in brackets like this: (c,m). A set of two numbers is used to characterize a mode shape, where c represents the number of sinusoidal waves in the circumferential (side view) direction and *m* represents the number of waves in the meridional (top view) direction [54]. This nomenclature applies well to tire modes where the belt structure is flexing. Some deviations from the rules apply when the belt structure moves like a rigid body. Detailed information about mode shape nomenclature for tires, including deformed plots from a finite element model that illustrate the axial, pitch, torsion, and diametric modes, can be found in [4].

In Table 3, conventional modal analysis results are presented in the second and third columns marked with "Accel." in the headers, as accelerometers were used for vibration measurement. Non-contact modal analysis results are given in the fourth and fifth columns marked with "SLDV" in the headers, as the SLDV system was used for vibration measurement. Natural frequencies and damping are listed for mode (0,0) axial through mode (7,0). Natural frequencies obtained by both measurement systems were very close, with SLDV frequencies within 3% of conventional frequencies. In every case the SLDV frequencies were slightly lower than the conventional frequencies. Damping was also very similar comparing the two measurement systems. Damping was typically around two or three percent, which is consistent with previous experience [55].

As the modal analysis results from the SLDV system are very similar to the conventional results, it is evidently possible to perform free tire modal analysis using an SLDV system instead of using accelerometers. This conclusion is based on the accuracy of the natural frequencies and mode shapes, assuming that the conventional method produces the ground truth. Note from Table 3, however,

FIGURE 10 SLDV measurement setup in the chassis dynamometer environment for the rotating testing. The single-point reference laser is second from left. The laser tachometer is located at front on a short tripod.

that the SLDV system did not identify as many modes as the conventional approach. Of the 16 modes listed in Table 3, 13 were identified using the conventional approach and nine were identified using the SLDV method. Mode shapes were identified by inspection using the Polytec Scanning Vibrometer (PSV) version 10.2 software. Identification of fewer tire modes with the SLDV system compared to the conventional accelerometer approach was most likely due to PSV software limitations, including difficulty in displaying and visualizing mode shapes. Of all the boundary conditions tested, the free condition was the most similar between the two measurement methods. The bungee cord restraint system was very similar in both tests. Only the excitation method differed, with an impact hammer used with the accelerometers and an electrodynamic shaker used with the SLDV system. It is reasonable to believe that the excitation was similar and sufficient in both tests. Thus, this leaves software limitations as a more likely reason for fewer modes being found in the SLDV test.

A graph displaying mobility versus frequency for the SLDV free measurement as calculated by the PSV

FIGURE 11 SLDV scan points in the chassis dynamometer environment for the rotating testing.

software is shown in Figure 12. Curves are shown in the three measurement directions, with the Y-direction being axial, and the X- and Z-directions being in the plane of the tire. The curves represent an average of the scan point measurements. While there are clearly resonant peaks in the curves of Figure 12 below 250 Hz, as expected, in practice it was difficult to identify and name mode shapes using the PSV software. A factor in this is the marginal appearance of the color contour plots that are produced by the software. These plots have a disorganized appearance. An example is the contour plot of free mode (2,0) in Figure 13. The inconsistent arrangement of scan point locations leads to a choppy-looking contour plot that hinders visualization of the modes. After the physical testing in this study was complete, Polytec suggested that a finite element model of the tire structure should have been made in advance of the testing. The idea would be to create a template that can be used to neatly define the SLDV scan points in a regular pattern, by essentially determining the measurement points (finite element nodes) in advance and using them as a guide during the scan point selection process. Following this procedure could conceivably result in improved quality contour plots that would enable better visualization of the tire modes, although that hypothesis was not tested.

6.2. Fixed Modes

Mode shapes and associated natural frequencies for the tire with fixed boundary conditions are listed in Table 4. In Table 4, conventional modal analysis results are presented in the second and third columns, and non-contact modal analysis results are given in the fourth and fifth columns. Natural frequencies and damping are listed for mode (0,0) axial through mode (7,0). Natural frequencies obtained by both measurement systems were very close, with SLDV frequencies at most 2% less than conventional frequencies. The sole exception was the (1,0) diametric mode, which was found to be 6% higher using the SLDV system. Damping was also very similar when comparing the two measurement systems. Damping was typically from two to four percent, which is expected. Again, the singular exception was the (1,0) aiametric mode, which was found to have 6.7% damping with the SLDV system, as opposed to 3.5% damping with the conventional system.

While natural frequencies and damping were similar for the fixed boundary conditions regardless of measurement method, the SLDV system did not identify as many modes as the conventional approach. This result was similar to the free boundary conditions case. It should be noted, however, that the shaker excitation method was different in the conventional and SLDV tests, which could explain why some modes were not identified using the SLDV measurement approach. In particular, a customary electrodynamic shaker was used in the fixed boundary conditions test with the SLDV system, whereas

TABLE 3 Natural frequencies and damping ratios for two modal analysis tests with free boundary conditions.

Mode shape	Accel. frequency (Hz)	Accel. damping (%)	SLDV frequency (Hz)	SLDV damping (%)	Frequency change (%)
(0,0) Axial	51.3	1.9	50.3	1.5	–2
(1,1) Pitch	78.6	2.8	N/A	N/A	N/A
(0,0) Torsion	N/A	N/A	N/A	N/A	N/A
(1,0) Diametric	88	2.7	N/A	N/A	N/A
(2,1)	76.9	2.3	76	2.8	–1
(2,0)	84.2	2.2	82.8	2.7	–2
(3,0)	104.1	1.7	101.5	1.7	–2
(3,1)	121.8	3.1	N/A	N/A	N/A
(4,0)	125.6	1.6	122.3	1.9	–3
(4,1)	150.2	2.9	N/A	N/A	N/A
(5,0)	148.2	1.8	144.3	2.3	–3
(5,1)	N/A	N/A	N/A	N/A	N/A
(6,0)	170.4	1.6	166.8	3.6	–2
(6,1)	N/A	N/A	N/A	N/A	N/A
Tire air cavity (TAC)	173.3	0.2	174	1.1	0
(7,0)	N/A	N/A	188.3	4.8	N/A

FIGURE 12 Mobility versus frequency with free boundary conditions.

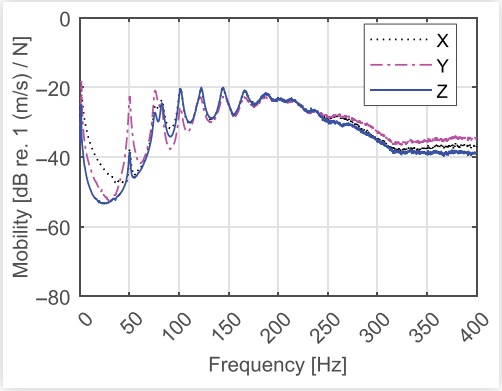

FIGURE 13 Free (2,0) mode with frequency = 82.8 Hz, physical measurement using SLDV. The undeformed shape is shown with a black color wireframe.

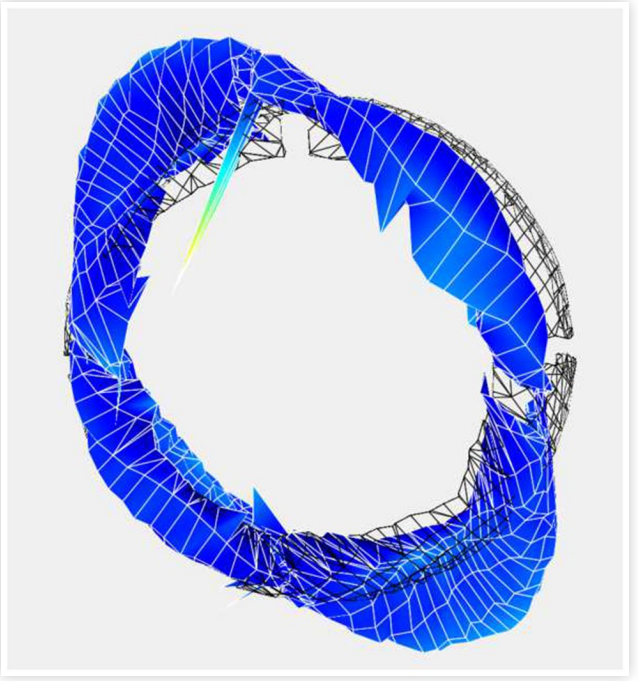

an integral shaker was used in the fixed test with the accelerometers. Despite the apparent disadvantages of the integral shaker, such as the possibility of undesirable dynamic interactions between the tire and the shaker itself, the test method involving the integral shaker and the accelerometers still identified more tire modes than the SLDV system did.

Of the 16 modes listed in Table 4, 13 were identified using the conventional approach and nine were identified using the SLDV method. Interestingly, the modes that were "missing" from the fixed SLDV test results were not the same as the modes that were absent from the free SLDV test results. For example, the (1,1) pitch mode was observed in the fixed modal analysis with a frequency of 45.5 Hz. This mode was not observed in the free modal analysis. A graph displaying mobility versus frequency for the SLDV fixed measurement, as calculated by the PSV software, is shown in Figure 14. Curves are shown in the three measurement directions, with the Z-direction being axial, and the X- and Y-directions being in the plane of the tire. The curves represent an average of the scan point measurements. In Figure 14, the expected change in tire vibratory response can be seen around 250 Hz, with highly damped modes appearing above this frequency.

6.3. Loaded Modes

Mode shapes and associated natural frequencies for the tire with loaded boundary conditions are listed in Table 5. In Table 5, conventional modal analysis results are presented in the second and third columns, and non-contact modal analysis results are given in the fourth and fifth columns. Natural frequencies and damping are listed for loaded mode (0,0) axial 1 through loaded mode (7,0) 2, for a total of 32 loaded modes. This is twice as many modes compared to the fixed and free cases. These results reflect a known phenomenon, whereby some of the modes may be "split," or they may separate into two modes by the flattened contact patch and associated loss of geometrical symmetry [56]. Both of the split modes, lower and higher in frequency, are listed in Table 5 with the "1" and "2" designations after the mode descriptions. Similar to the other boundary condition cases, the SLDV measurement method did not find as many modes as the conventional approach. Furthermore, in some cases, the SLDV result did not identify both of the split modes, but rather just one of them. For example, the (4,1) 1 mode was found in the SLDV data with a frequency of 132.0 Hz, but the (4,1) 2 mode was not observed.

Natural frequencies obtained by both measurement systems were close, with SLDV frequencies within 5% of the conventional frequencies. The sole exception was the (1,1) Pitch 1 mode, which was found to be 7% lower using the SLDV system. Damping was also very similar when comparing the two measurement systems. Damping was typically from two to four percent, which is expected. Again, the singular exception was the (1,1) pitch 1 mode, which was found to have 5.6% damping with the SLDV system, as opposed to 1.4% damping with the conventional system. While natural frequencies and damping were similar for the loaded boundary conditions regardless of the measurement system, the SLDV system did not identify as many modes as the conventional approach. This result was similar to the other boundary conditions cases. Of the 32 modes listed in Table 5, 24 were identified using the conventional approach and 13 were identified using the SLDV method.

One factor that may be relevant to the identification of tire modes in the loaded boundary conditions case is that the tire environment was markedly different in the

TABLE 4 Natural frequencies and damping ratios for two modal analysis tests with fixed boundary conditions.

Mode shape	Accel. frequency (Hz)	Accel. damping (%)	SLDV frequency (Hz)	SLDV damping (%)	Frequency change (%)
(0,0) Axial	38.8	1.5	38	3.3	–2
(1,1) Pitch	46.2	2	45.5	3.8	–2
(0,0) Torsion	N/A	N/A	N/A	N/A	N/A
(1,0) Diametric	60.1	3.5	63.5	6.7	6
(2,1)	78.1	2.3	N/A	N/A	N/A
(2,0)	84.1	2.2	84	2.4	0
(3,0)	104	1.7	102.5	2.4	–1
(3,1)	120.2	2.8	N/A	N/A	N/A
(4,0)	125.6	1.7	123	3	–2
(4,1)	153.8	3	N/A	N/A	N/A
(5,0)	148.8	1.9	146	3.1	–2
(5,1)	N/A	N/A	N/A	N/A	N/A
(6,0)	170.3	1.4	169	2.7	–1
(6,1)	179.9	2.6	N/A	N/A	N/A
Tire air cavity (TAC)	N/A	N/A	N/A	N/A	N/A
(7,0)	N/A	N/A	189.5	2.5	N/A

conventional modal analysis test compared to the non-contact test using the SLDV system. The conventional test was conducted on a rig that tested and loaded only the tire and wheel in isolation. The SLDV test, however, was conducted in a chassis dynamometer test cell with the tire and wheel attached to a vehicle. In the circumstances of the conventional test, it is reasonable to believe that the integral shaker provided sufficient excitation, especially since it previously did so in the fixed (no footprint contact) boundary conditions case. However, the electrodynamic shaker (more sized for component-level testing) that was used in the SLDV test may not have been able to provide enough energy to the tire, wheel, and vehicle system to excite as many tire modes as desired. Regarding the difference in the (1,1) pitch 1 mode natural frequency, it is possible that the value from the SLDV test was lower than the conventional test since the vehicle's flexibility, including its suspension compliances, may have affected the (1,1) pitch 1 mode and lowered its frequency. The conventional test involving accelerometers would have had a stiffer environment, as the tire and wheel were attached to a test rig only, resulting in a higher (1,1) pitch 1 natural frequency.

FIGURE 14 Mobility versus frequency with fixed boundary conditions.

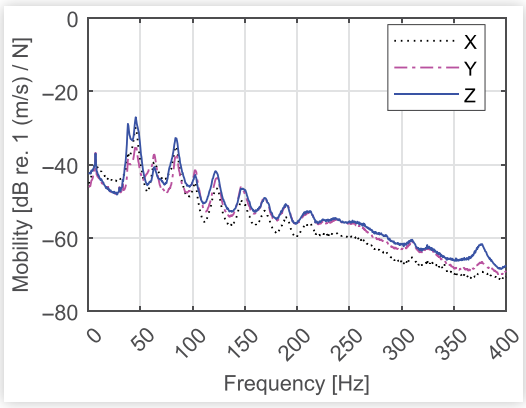

A graph displaying mobility versus frequency for the SLDV-loaded measurement, as calculated by the PSV software, is shown in Figure 15. Curves are shown in the three measurement directions, with the Z-direction being axial, and the X- and Y-directions being in the plane of the tire. The curves represent an average of the scan point measurements. In this loaded case, the tire modes are damped significantly above 200 Hz, with lightly damped modes occurring below 120 Hz, and moderately damped modes appearing between these two frequencies.

Figure 16 is a bar graph depicting the first five modes that were found in all three non-rotating boundary conditions using the conventional modal analysis measurement method. Figure 17 depicts the sixth through eleventh modes that were found. Note that in the loaded case, the lower-frequency mode (of a mode pair) is presented in the graph for the modes where the mode is separated and two frequencies were identified. From Figures 16 and 17, it can be seen that the conventional measurement process consistently identified 11 modes in a frequency range from 0 to 200 Hz. Starting with mode (2,1) and up, frequencies were similar between the three boundary conditions, with the difference in frequencies between free and fixed states within a few percent in most cases. The fixed condition compared to the free condition led to reduced resonant frequencies for the initial modes, while the impact of changes to boundary conditions became progressively less significant for higher-order modes. The lowest frequency modes, namely the (0,0)

TABLE 5 Natural frequencies and damping ratios for two modal analysis tests with loaded boundary conditions.

Mode shape	Accel. frequency (Hz)	Accel. damping (%])	SLDV frequency (Hz)	SLDV damping (%)	Frequency change (%)
(0,0) Axial 1	42.1	1.6	41.5	5.1	–2
(0,0) Axial 2	N/A	N/A	N/A	N/A	N/A
(1,1) Pitch 1	48.1	1.4	44.5	5.6	–7
(1,1) Pitch 2	N/A	N/A	N/A	N/A	N/A
(0,0) Torsion 1	52.5	3.1	N/A	N/A	N/A
(0,0) Torsion 2	64.7	1.7	N/A	N/A	N/A
(1,0) Diametric 1	65.4	2.5	N/A	N/A	N/A
(1,0) Diametric 2	76.6	3.1	N/A	N/A	N/A
(2,1) 1	72.5	2.1	70.8	2.8	–2
(2,1) 2	88.8	2.7	88.5	2.7	0
(2,0) 1	83.4	3.2	N/A	N/A	N/A
(2,0) 2	91.7	1.9	N/A	N/A	N/A
(3,0) 1	103.5	1.7	100.3	2.6	–3
(3,0) 2	114.6	1.6	110.0	2.7	–4
(3,1) 1	118.1	0.7	N/A	N/A	N/A
(3,1) 2	129.1	2.5	N/A	N/A	N/A
(4,0) 1	126.2	1.6	N/A	N/A	N/A
(4,0) 2	138.5	1.7	N/A	N/A	N/A
(4,1) 1	134.1	1.4	132.0	3.1	–2
(4,1) 2	154.1	2.7	N/A	N/A	N/A
(5,0) 1	149.6	1.0	142.5	1.3	–5
(5,0) 2	156.9	0.1	154.0	2.5	–2
(5,1) 1	N/A	N/A	N/A	N/A	N/A
(5,1) 2	N/A	N/A	N/A	N/A	N/A
(6,0) 1	161.7	1.7	165.0	2.5	2
(6,0) 2	167.6	0.5	N/A	N/A	N/A
(6,1) 1	171.4	1.6	N/A	N/A	N/A
(6,1) 2	N/A	N/A	N/A	N/A	N/A
Tire air cavity (TAC) 1	173.9	2.1	174.5	2.7	0
Tire air cavity (TAC) 2	N/A	N/A	N/A	N/A	N/A
(7,0) 1	N/A	N/A	188.3	2.4	N/A
(7,0) 2	N/A	N/A	203	3.8	N/A

axial, (1,1) pitch, and (1,0) diametric modes, showed the biggest differences in frequency across boundary conditions. For example, the (0,0) axial mode, in which the sidewall deformations are high and the belt reinforcements essentially translate as a rigid body along the axle of the "vehicle," the free frequency was more than 20% higher than the fixed and loaded frequencies. Note that in the case of the (0,0) axial mode, a second higher frequency was not identified in loaded testing.

Figure 18 is a bar graph depicting the modes that were found in all three non-rotating boundary conditions using the SLDV modal analysis measurement method in a 0–200 Hz frequency range. Five modes were identified using the SLDV measurement process, as opposed to the 11 modes that were identified using the conventional method. In general, fewer modes were identified using the SLDV system compared to the measurement approach using accelerometers. Overall trends were similar comparing both measurement methods, however. Starting with mode (3,0) and up, SLDV frequencies were within a few percent of one another, regardless of boundary condition. Fixed frequencies were slightly higher than free frequencies, with the exception of the (0,0) axial mode. In that case, the free frequency was more than 30% higher than the fixed or loaded frequencies. The second (0,0) axial mode for the loaded boundary condition was not identified using either measurement technique. The free (0,0) axial mode had a 2% lower frequency with the SLDV measurement system compared to the conventional system.

6.4. Rotating Operating Deflection Shapes

Mode shapes were difficult to determine in the rotating condition. Only the 30 MPH case produced usable data, and in this case, three modes were clearly identified that

FIGURE 15 Mobility versus frequency with loaded boundary conditions.

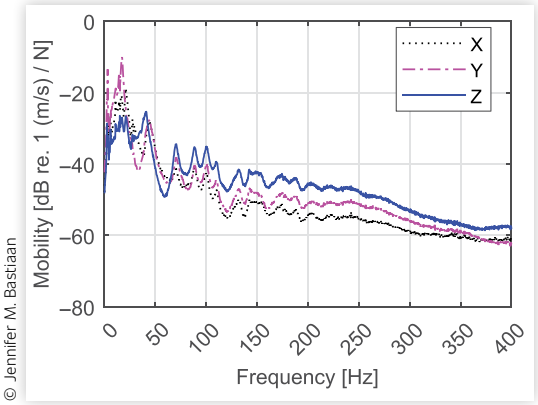

were previously measured in the non-rotating boundary conditions. A graph displaying velocity versus frequency for the SLDV rotating measurement, as calculated by the PSV software, is shown in Figure 19. Curves are shown in the three measurement directions, with the Z-direction being axial, and the X- and Y-directions being in the plane of the tire. The curves represent an average of the scan point measurements. In general, peaks in the rotating curves are not very clear in comparison with the peaks in the curves from the non-rotating conditions, as shown in Figures 12, 14, and 15. However, a few clear resonant peaks appear in the rotating curves below 200 Hz in Figure 19. These peaks are associated with modes (3,0), (5,0), and (6,0), as illustrated in the bar graph of Figure 20. In this graph, the loaded modes represent the lower frequency of the split pair, for the scenarios where both frequencies were identified. For the rotating modes, only one frequency of the pair (as shown) was identified in the results. As can be seen in Figure 19, peaks associated with tire rotating modes are not as clearly delineated as in the other non-rotating boundary conditions. Furthermore, damping in the modes above 250 Hz appears to be lower than in the other boundary conditions.

It is interesting to see how significantly the frequencies dropped for the three modes of Figure 20 in the rotating boundary conditions compared to the other three non-rotating boundary conditions. Generally, the frequencies for the non-rotating boundary conditions were very similar, within 3%. However, the rotating frequency decreased from the loaded frequency by up to 19%, in the case of the (5,0) mode. This change may be a product of a spin softening effect during rotation, wherein a rotating structure such as a tire can lose stiffness compared to its non-rotating operating condition due to the presence of centrifugal forces. One investigation into the spin softening effect on a rotating flexible steel blade found that each of the first five natural frequencies was reduced by more than 5% when the blade was rotating at 4,775 RPM compared to when it was at rest [57]. Comparable studies are harder to find for tires and other structures with a considerable elastomer material component. However, one study specific to tires reported that a drop in frequency of about 10% for lower-frequency in-plane normal modes can be expected in the transition from non-rolling to rolling [58]. Therefore, the observation of reduced natural frequencies for rotating tires compared to non-rotating tires in the current study is consistent with published research results.

FIGURE 16 Tire modes common to all three boundary conditions without rotation, first through fifth, physical measurement using accelerometers.

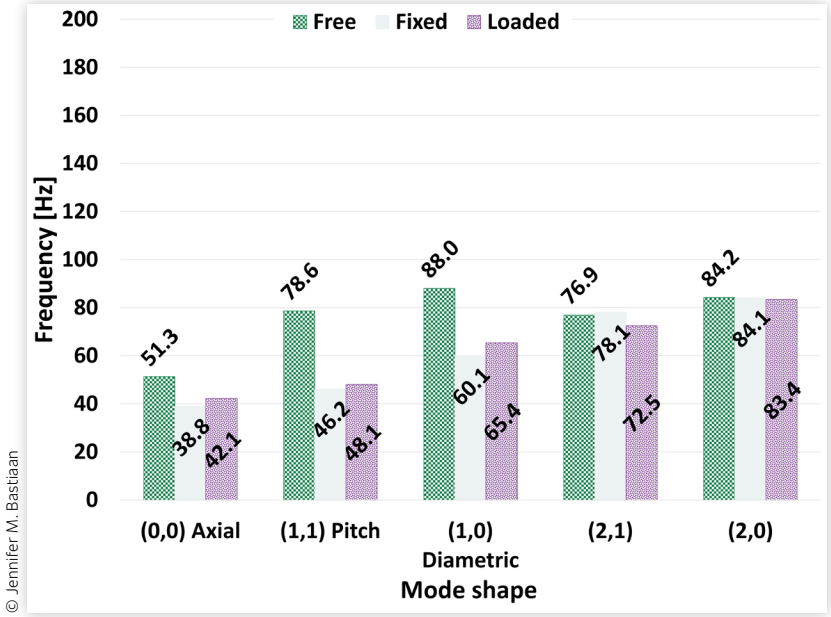

FIGURE 17 Tire modes common to all three boundary conditions without rotation, sixth through eleventh, are physical measurements using accelerometers.

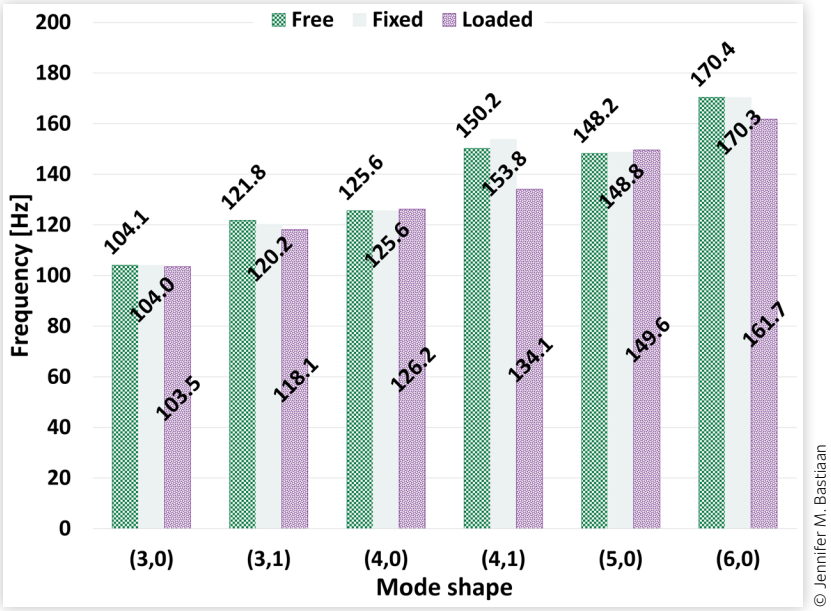

Additionally, the temperature of the tire may have been a factor in the measured results. By the time of the 30 MPH measurement, that produced the results of Figure 20, the vehicle had been running hard on the chassis dynamometer all day, meaning that the tires were probably very warm during the 30 MPH test. The elastomer materials used in a tire are known to have temperature- and frequency-dependent properties, in terms of both stiffness and damping. Certain rubbers, for example, have a shear storage modulus and loss factor that are highly dependent on temperature, which can lead to consequential differences in behavior depending on temperature [59]. In one material testing study, a tire rubber compound was found to have a reduced elastic modulus with increased temperature, with a decrease of about 60% in elastic modulus from 20°C (at room temperature) to 60°C (at an elevated tire operating temperature) [60]. While this result was for a rubber compound only, which may only be one part of the complex non-linear system that is a tire, it illustrates that the static stiffness of an important tire material component can be reduced significantly with a pronounced increase in temperature. As the static stiffness of tire rubber decreases with increased temperature, it is likely that tire modal frequencies will also decrease with increased tire operating temperature.

It is conceivable that the tire in a rotating test with a high operating temperature was significantly more compliant compared to the same tire in a loaded test (vehicle parked, not moving) at room temperature. Furthermore, it is possible that rotation exacerbates the frequency split in the loaded modes, with the lower frequency decreasing further, and the higher frequency increasing further. Finally, the compliance in the vehicle's suspension systems may also be a factor in lowering the frequencies during rotation, although it should be noted that these effects may be represented to some extent in the loaded case, except for temperature effects on suspension bushings.

Figures 21–23 show color contour plots for the three modes that were measured by the SLDV system for all boundary conditions investigated. Figure 21 depicts the (3,0) mode, Figure 22 highlights the (5,0) mode, and Figure 23 illustrates the (6,0) mode. A review of the mode shapes emphasizes the quality issue with the images from the PSV software. The free and fixed boundary conditions produced the lowest quality images. The testing in these scenarios involved scanning sections of the tire and merging the results afterward. This procedure resulted in disconnected contour plots, especially in the fixed boundary conditions case. Contour plots from the loaded and rotating conditions were better, as only the tire sidewall was measured in the chassis dynamometer environment, without any post-processing or stitching of results afterward. Still, these boundary conditions also produced disappointing mode shape plots that made it difficult to visualize and understand the modes in some cases.

7. Discussion

While three modes of vibration were identified using the SLDV measurement method in all four boundary conditions tested, including free, fixed, loaded, and rotating,

FIGURE 18 Tire modes common to all three boundary conditions without rotation are physical measurement using SLDV.

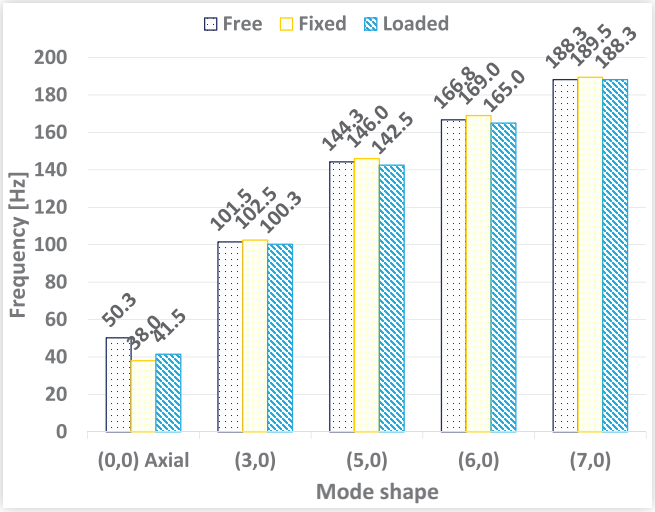

not as many modes were recognized as was expected (or hoped for). A comparison of the total number of modes found up to the (7,0) mode for both the conventional (accelerometers) and the non-contact (SLDV) test methods appears in Table 6. The boundary conditions listed are for free, fixed, and loaded, which were the three conditions in which both measurement methods were used. From Table 6 it can be seen that the non-contact measurement method using SLDV consistently identified fewer modes than the conventional method using accelerometers. There were a number of issues that may be related to this, which are enumerated here, along with a discussion of next steps. The list of issues and suggested future work is presented in order of priority, with the top items most likely to generate new knowledge about tire ODS measurement using a SLDV system.

FIGURE 19 Velocity versus frequency with rotating boundary conditions, 30 MPH vehicle speed.

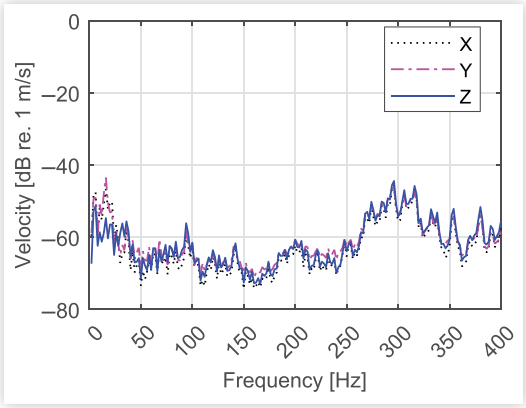

7.1. SLDV Rotating Tire Test Issues and Next Steps

7.1.1. Time Data Not Recorded by SLDV System—Add Time Data Acquisition The data acquisition system shipped with the SLDV system cannot record time data in a running sense. That is, it is not possible to start recording a sensor signal at the start of a test and record it continuously until the end of the test. Therefore, the once-per-rev optical tachometer data that was included in this study was not properly recorded, and it could not be used in any sort of post-processing. Such a signal would be required to "de-rotate," or otherwise remove, rigid body rotation from the recorded vibration data. Going forward, an auxiliary data acquisition system should be added to the test setup that is time-stamped relative to the main SLDV data acquisition system. Such tachometer data could, at the very least, be used monitor the rotational speed of the system.

7.1.2. Rotating Speed Inconsistency—Add Encoder for Monitoring The SLDV system, as delivered, was designed to measure rotating vibration under the assumption of consistent rotating speed. As not many modes were measured during the rotating operation of the tire in this study, the question of rotational speed consistency arose. It is possible that the front axle of the test vehicle did not maintain a sufficiently consistent rotating speed during chassis dynamometer testing. However, this issue is impossible to investigate retroactively, as the optical tachometer data was not recorded properly by the SLDV system. In the future, the angular position and angular velocity of the tire should be measured with a rotary encoder, along with the SLDV vibration data to confirm steady-state operation. Ideally, a dedicated encoder that can output at least 128 pulses per wheel revolution should be used, such that longitudinal slip can be monitored. Additionally, a method for indicating a once-per-wheel-revolution angular position index is required. Moreover, the rotating tire test should be conducted on a dedicated tire dynamometer, where the tire and wheel are isolated during the test, and there is no vehicle to add to any inconsistency in speed.

7.1.3. Poor Quality Mode Shape Plots—Define Scan Points with a Finite Element Mesh Image quality from the PSV software was barely adequate, making it difficult to visualize modes, and raising the possibility that they were too poorly presented to be seen. To address this concern, Polytec stated that a finite element model of the tire structure should be created in advance of the measurements, for the purpose of defining a regular measurement grid. The idea would be to create a simple finite element model with a regular quadrilateral mesh defined at the exterior boundary of the tire. The nodes of this mesh would be used to define the scan points for

FIGURE 20 Tire modes common to all four boundary conditions including rotation are physical measurements using SLDV.

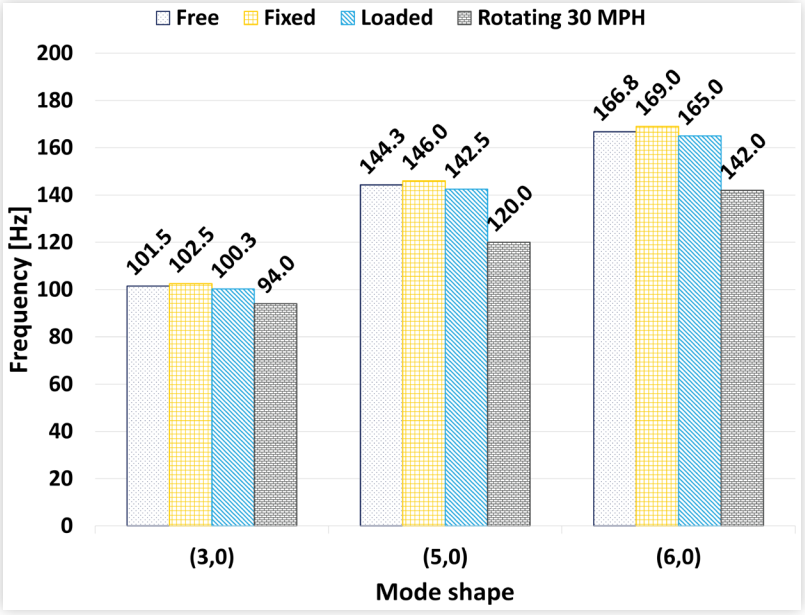

FIGURE 21 SLDV measurement of tire mode (3,0).

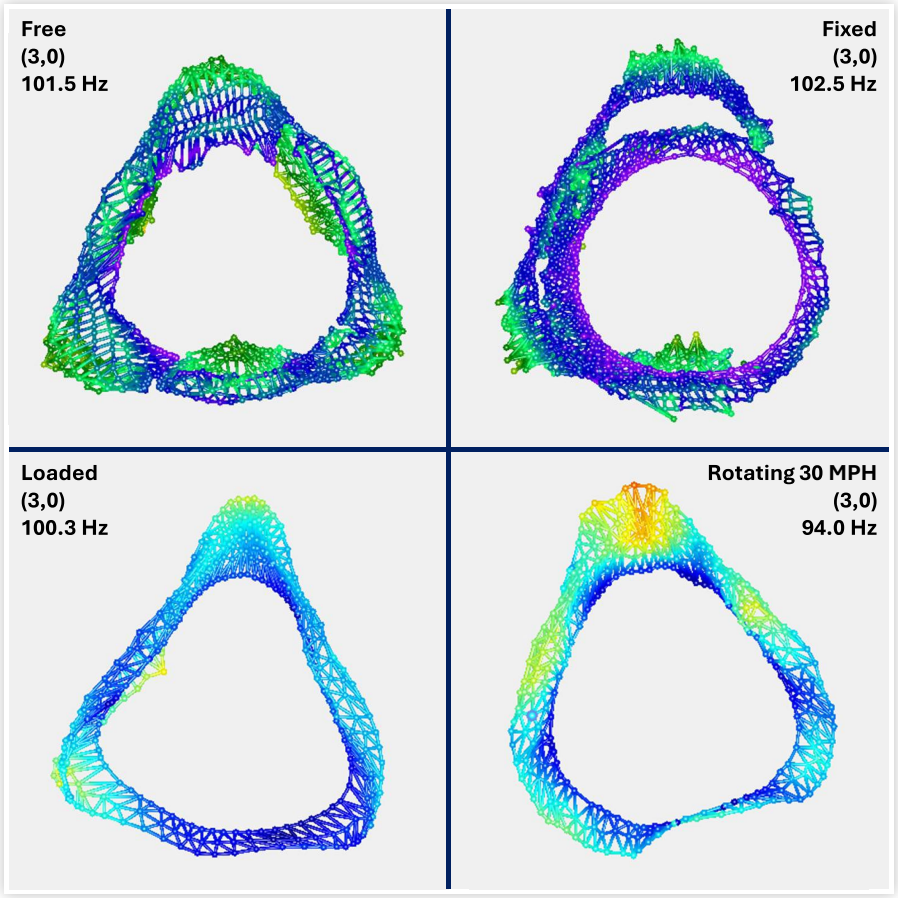

FIGURE 22 SLDV measurement of tire mode (5,0).

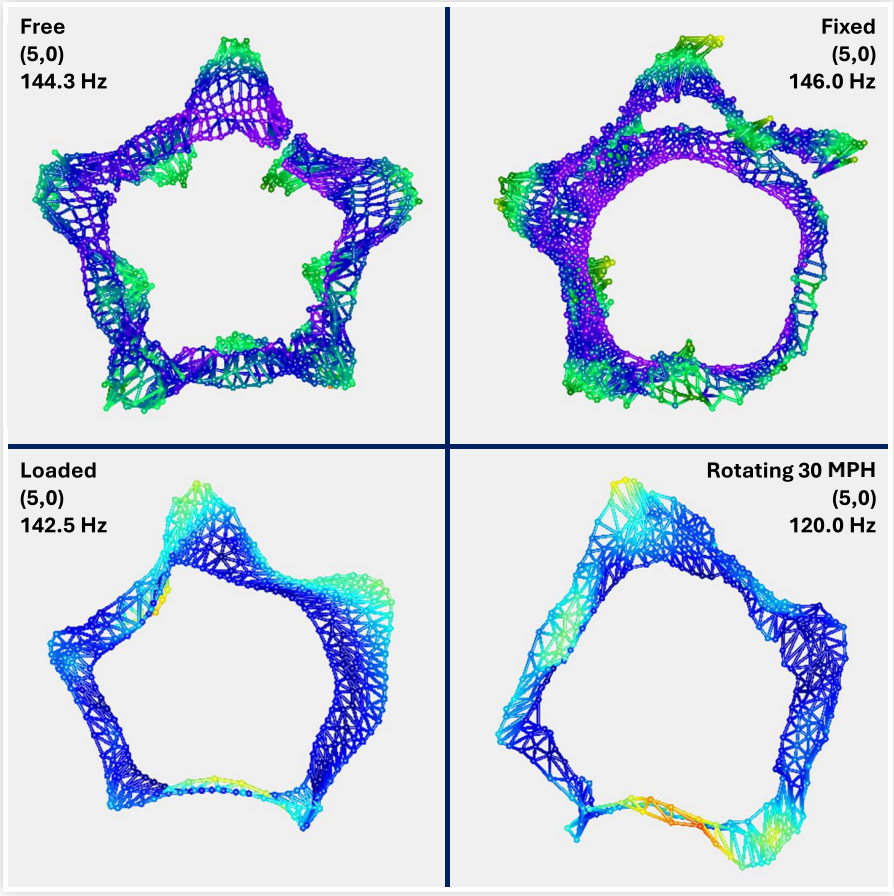

the SLDV system, which should, in turn, produce professional-quality contour plots.

7.1.4. No Tire Temperature Measurement—Add Thermocouples Significant decreases in tire natural frequencies were observed with operating rotating boundary conditions, in comparison with non-rotating conditions. The temperature of the tire under test may be associated with this behavior. Future operating tire tests should include thermocouples, at least two, with one installed near the tire sidewall and the other near the tire tread. These sensors would be used to measure operating temperatures, with the goal of understanding the influence of temperature on the rotating modes of vibration.

7.1.5. Insufficient Excitation during Rotation—Add More Powerful Inputs An open question is whether there was sufficient input excitation to the tire in the chassis dynamometer environment. The right front drum of the chassis dynamometer was finished with a fine knurled surface that, in itself, may not have been sufficient to excite many modes of vibration. Thus, the chassis dynamometer test was a simulation of straight-line vehicle operation on a very smooth road. An experiment was conducted during dynamometer testing in which an electrodynamic shaker was attached to the right front vehicle suspension during tire rotation, thus supplying supplementary excitation. Results showed that this particular shaker made very little difference, as more modes were not revealed by its addition. It may have been too small to provide a substantive force in the context of vehicle operation. Some possibilities for future work include impact excitation by attaching a cleat to the drum [61], or possibly by striking the system with a hammer or projectile.

7.1.6. Steady-State Measurement Limitation—Test More Steady-State Speeds It is important to emphasize that the SLDV system can be used for measuring the vibration of structures undergoing steady-state rotation only. As a result, a consistent angular velocity is necessary when employing the Eulerian approach with SLDV to accurately measure the Operating Deflection Shapes of a rotating tire. SLDV cannot be used for measuring the vibration of structures undergoing changes in rotational speed. At the beginning of the chassis dynamometer testing performed during this study, a number of speed sweeps were performed with the vehicle. None of this sweep data could be used, as there was no way to post-process the data to extract any meaning from it. This is

FIGURE 23 SLDV measurement of tire mode (6,0).

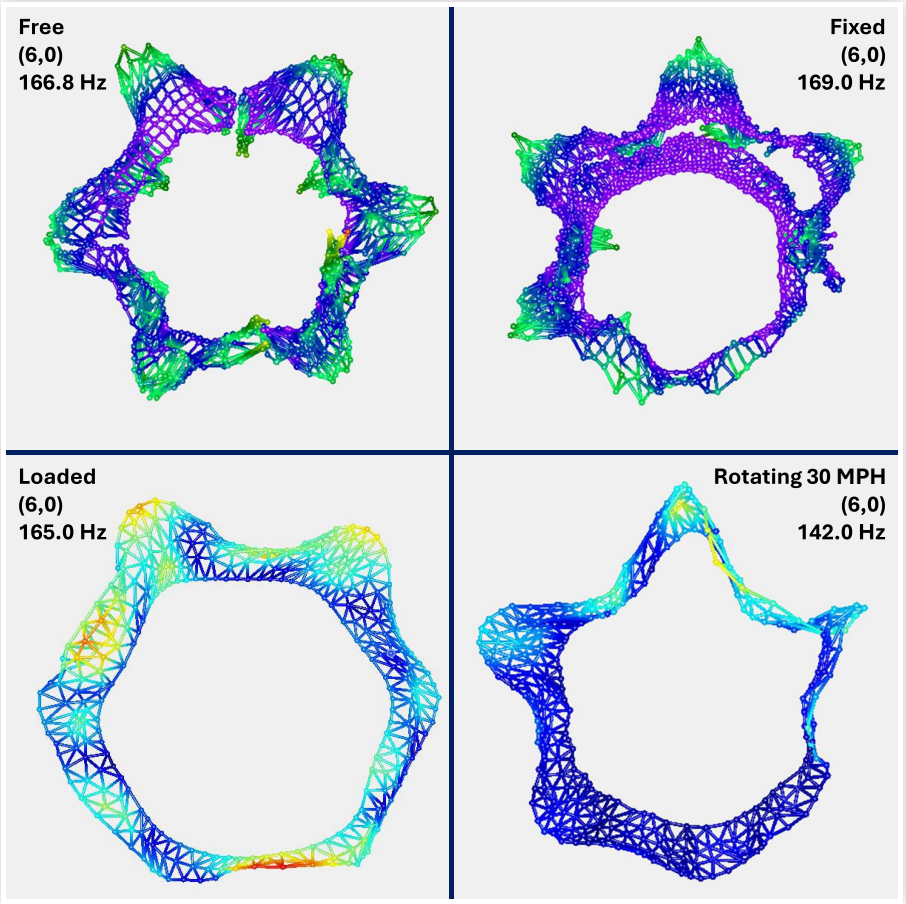

a noteworthy limitation of the SLDV measurement system that was employed. However, more work should be done to extend the current study from its steady-state rotating condition of 30 MPH. More steady-state speeds should be tested to investigate how the tire's natural frequencies change with operating speed.

7.2. Tire Operating Modes Measurement Methods Comparison

The two most important methods for non-contact measurement of operating tire modes are SLDV and DIC. A comparison of these approaches for measuring the modes of a rotating tire appears in Tables 7 and 8. The observations that appear in Tables 7 and 8 are based on the experimental mechanics research experiences of the authors, who have also used DIC to measure tire normal modes during rotation [30]. In addition to information about SLDV and DIC, details are provided about the conventional measurement approach using vibration sensors that make contact with the tire under test. Regarding the instrument cost of acquiring a SLDV or DIC measurement system, a complete SLDV system will cost approximately three times as much as a DIC system, depending on the number of non-contact vibration measurement devices (laser vibrometers, cameras) and whether commercial or custom software is used with the systems.

TABLE 6 Number of tire normal modes identified up to the (7,0) mode, depending on measurement method.

Boundary condition	Accelerometers	SLDV	Difference
Free	13	9	–4
Fixed	13	9	–4
Loaded	24	13	–11

While there are many advantages and disadvantages of each measurement approach, the ease of SLDV measurement stands out as a plus. There is no real post-processing required with the SLDV approach, other than having a human operator inspect the results to identify mode shapes. The automated nature of the process is also ironically its disadvantage, as there is no (straightforward) way to go back and correct the results with measured information about rotating speed. In that sense, DIC seems attractive, as that method can consider changes in rotational speed including measurement of intentionally transient events. However, this comes with

TABLE 7 Comparison of tire operating modes measurement methods—part A.

Characteristic	Pointwise sensors (accelerometers, strain gauges)	Laser Doppler Vibrometer (LDV)	Digital Image Correlation (DIC)
Contact vs. non-contact	- Contact-based: Requires physical attachment to the tire	- Non-contact: Suitable for rotating tires if optical access is available	- Non-contact: Ideal for rotating tires if cameras have lines of sight
	- Wiring complicates the use of rotating tires	- No need for attachment or wiring	- No need for physical attachment
Setup and mounting	- Sensors must be attached at points of interest	- Requires three heads for 3D measurement	- Requires stereo cameras for 3D coverage
	- Requires cabling, slip rings, or telemetry for data transfer	- Can operate in single-point or scanning mode	- Needs a speckled pattern or markers on the tire
	- Possible mass-loading on the tire	- Requires precise alignment and line of sight to the tire surface	- Consistent lighting and camera placement are crucial
Data coverage and resolution	- Pointwise: Data only at sensor locations	- Potentially high spatial resolution if scanning multiple points	- Full-field: Captures data across the visible surface
	- Limited spatial coverage	- Single-point LDV provides data at the measured spot	- Spatial resolution depends on camera quality and field of view
		- Can readily measure the sidewall and the parts of the tread area using the Eulerian method	- Because it uses a tracking approach, typically it only measures sidewall
Frequency range	- Wide range of measurable frequencies (depends on transducer choice)	- Extremely wide frequency range	- Generally well-suited for low-to-mid frequencies
		- Sensitive to very high frequencies	- High-speed cameras can capture higher frequencies but generate large data volumes
Rigid body vs. flexible modes	- Can capture both rigid body and some flexible modes	- Excellent for measuring flexible modes	- Captures both rigid body and flexible modes across the full-field
	- Multiple sensors are needed to reconstruct complex modes	- Less suited for purely rigid body motion (high sensitivity to relative velocity)	- Especially good for large/complex deformations

TABLE 8 Comparison of tire operating modes measurement methods—part B.

Characteristic	Pointwise sensors (accelerometers, strain gauges)	Laser Doppler Vibrometer (LDV)	Digital Image Correlation (DIC)
Measurement and processing speed	- Fast acquisition (time-domain or real-time possible)	- Rapid acquisition in single-point mode	- Camera-based measurement can be fast
	-Minimal post-processing needed	- Scanning approach adds measurement time; however, data processing is typically straightforward	- Post-processing can be time-consuming
Data volume	- Relatively small (few channels)	- Moderate (single-point or scanning methods)	- Large data sets for full-field measurements, especially with high-speed or high-resolution setups
Calibration sensitivity	- Straightforward sensor calibration	- Extremely sensitive to alignment, standoff distance, and setup	- Requires careful system calibration
	- Mounting changes can affect accuracy slightly	- Rigid body motion of the tire can affect the measurement	- Can handle rigid body motion well
Cost and complexity	- Generally inexpensive per sensor	- Typically, higher costs for hardware	- High equipment cost (cameras and lighting)
	- Cost rises if many sensors are needed	- Complex alignment requirements for rotating tires	- Complexity increases with desired resolution, number of cameras, and processing speed
Suitability for rotating tires	- Feasible, but wiring and attachments can be problematic	- Capable of full-field measurement of rotating tires	- Capable of full-field measurement of rotating tires
	- Potential alteration of tire behavior due to added mass	- Alignment and optical access are critical	- Requires careful camera placement, pattern application, and illumination
		- Needs a very constant rotation speed for the duration of scanning (e.g., 15 min)	- Does not need constant rotation speed and can capture data quickly
			- Can readily measure transient events

an opportunity cost, as the DIC test is not really over when it is over. Once the measurement phase is finished, the post-processing phase begins.

8. Conclusions

The results of this work show that a SLDV system is capable of measuring light truck tire modes of vibration in non-rotating boundary conditions, including fixed, free, and loaded. Results were similar to those from comparable modal analysis tests performed using conventional methods with accelerometers used for vibration measurement. Across boundary conditions, natural frequencies from the SLDV system were largely within three percent of the frequencies as measured using the conventional approach. Damping values were similar as well, with both modal analysis testing approaches producing values in the two to four percent range, which is an expected range for damping of tire modes.

The SLDV system was also able to measure some tire operating modes during rotation in a chassis dynamometer test environment. Three modes of vibration were observed in the rotating condition at 30 MPH, in particular the (3,0), (5,0), and (6,0) modes. These modes were also measured by the SLDV system in three non-rotating boundary conditions. Interestingly, the natural frequencies decreased by up to 19% once the tire was rotating, which may be due to spin softening, temperature effects, or other reasons related to geometrical modifications of the loaded tire.

While the tire operating modes that were measured are a compelling argument in favor of the SLDV measurement approach, more modes should have been clearly identified using the SLDV process. Future work should address concerns identified during this study, such as the need for testing at a consistent rotating speed and the addition of a stronger tire excitation system. Furthermore, time data from an encoder should ideally be recorded to monitor rotating speeds, and temperature sensors should be added to investigate thermal effects. The most important question remaining after the completion of this work, however, is this: Will a more consistent tire rotating speed lead to more and better modal analysis results? Only a detailed investigation of the rotating speed issue can answer this question.

Conflict of Interest

The authors and SAE International declare that one of the authors of this article is on the editorial board of the journal. SAE warrants that confidentiality was maintained throughout the peer-review process and no partiality was granted to the work. SAE further warrants that the editorial board member had no influence and did not take part in any type of decision-making or peer review.

Acknowledgements

This work was supported by Yokohama Tire Corporation of America (project agreement number 2402) and the U.S. National Science Foundation (award number 2320553). Special thanks to Sean Lee, Jim Cuttino, Jeremy Kahrs, and the Advanced Engineering team at Yokohama for their valuable insights and guidance. In addition, we would like to express our gratitude to Osama Jameel and Mazie Jackan of Polytec for providing technical support.

Contact Information

Jennifer Bastiaan, corresponding author
jbastiaan@kettering.edu

References

1. Carlier, M., "Leading Reasons Motivating the Purchase of Electric Vehicles According to Consumers Worldwide as of the First Half of 2024," Statista, accessed April 2025, https://www.statista.com/statistics/1314926/leading-motivator-to-ev-purchase-worldwide/.
2. Freeman, T. and Cerrato, G., "Vehicle Pass-by Noise Estimations for Component-Level Design," SAE Technical Paper 2011-01-1608 (2011), doi:https://doi.org/10.4271/2011-01-1608.
3. Goto, K., Kondo, T., Takahira, M., Umemura, E. et al., "Indoor Pass-by Noise Evaluation System Capable of Reproducing ISO Actual Road Surface Tire Noise," SAE Technical Paper 2016-01-0479 (2016), doi:https://doi.org/10.4271/2016-01-0479.
4. Wheeler, R., Dorfi, H., and Keum, B., "Vibration Modes of Radial Tires: Measurement, Prediction, and Categorization under Different Boundary and Operating Conditions," SAE Technical Paper 2005-01-2523 (2005), doi:https://doi.org/10.4271/2005-01-2523.
5. Braghin, F., Cheli, F., Melzi, S., Negrini, S. et al., "Experimental Modal Analysis and Modelling of an Agricultural Tire," in *Topics in Model Validation and Uncertainty Quantification, Volume 5: Proceedings of the 31st IMAC, A Conference on Structural Dynamics, 2013*, vol. 41 (New York: Springer, 2013), 213-220.
6. Kindt, P., De Coninck, F., Sas, P., and Desmet, W., "Experimental Modal Analysis of Radial Tires and the Influence of Tire Modes on Vehicle Structure-Borne Noise," SAE Technical Paper 2006-05-0087 (2006), doi:https://doi.org/10.4271/2006-05-0087.

7. Patil, K., Baqersad, J., and Behroozi, M., "Experimental Modal Analysis on a Tyre—Lessons Learned," *International Journal of Vehicle Noise and Vibration* 13, no. 3-4 (2017): 200-215.
8. Patil, K., Baqersad, J., and Bastiaan, J., "Effects of Boundary Conditions and Inflation Pressure on the Natural Frequencies and 3DMode Shapes of a Tire," SAE Technical Paper 2017-01-1905 (2017), doi:https://doi.org/10.4271/2017-01-1905.
9. Matsubara, M., Tajiri, D., Horiuchi, M., and Kawamura, S., "Evaluation of Spring Properties of Tire Sidewall under Changes in Inflation Pressure," *SAE Int. J. Passeng. Cars - Mech. Syst.* 8, no. 3 (2015): 825-833, doi:https://doi.org/10.4271/2015-01-2193.
10. Matsuzaki, R. and Todoroki, A., "Wireless Monitoring of Automobile Tires for Intelligent Tires," *Sensors* 8, no. 12 (2008): 8123-8138.
11. Bastiaan, J., Chawan, A., Eum, W., Alipour, K. et al., "Intelligent Tire Prototype in Longitudinal Slip Operating Conditions," *Sensors* 24, no. 9 (2024): 2681.
12. Baqersad, J., Poozesh, P., Niezrecki, C., and Avitable, P., "Photogrammetry and Optical Methods in Structural Dynamics—A Review," *Mechanical Systems and Signal Processing* 86, no. 8 (2017): 17-34.
13. Niezrecki, C., Reu, P.L., Baqersad, J., Rohe, D.P. et al., "DIC and Photogrammetry for Structural Dynamic Analysis and High-Speed Testing," in *Handbook of Experimental Structural Dynamics* (New York: Springer, 2022), 409-478.
14. Rothberg, S., Allen, M., Castellini, P., DiMaio, D. et al., "An International Review of Laser Doppler Vibrometry: Making Light Work of Vibration Measurement," *Optics and Lasers in Engineering* 99 (2017): 11-22.
15. Helfrick, M.N., Niezrecki, C., Avitabile, P., and Schmidt, T., "3D Digital Image Correlation Methods for Full-Field Vibration Measurement," *Mechanical Systems and Signal Processing* 25, no. 3 (2011): 917-927.
16. Peters, W.H. and Ranson, W.F., "Digital Imaging Techniques in Experimental Stress Analysis," *Optical Engineering* 21, no. 3 (1982): 427-431.
17. Sutton, M.A., Wolters, W.J., Peters, W.H., Ranson, W.F. et al., "Determination of Displacements Using an Improved Digital Correlation Method," *Image and Vision Computing* 1, no. 3 (1983): 133-139.
18. Chu, T., Ranson, W., and Sutton, M., "Applications of Digital-Image-Correlation Techniques to Experimental Mechanics," *Experimental Mechanics* 25 (1985): 232-244.
19. Schreier, H., Orteu, J.-J., and Sutton, M.A., *Image Correlation for Shape, Motion and Deformation Measurements: Basic Concepts, Theory and Applications* (New York: Springer-Verlag, 2009).
20. Panchal, R., Horton, L., Poozesh, P., Baqersad, J. et al., "Vibration Analysis of Healthy Skin: Toward a Noninvasive Skin Diagnosis Methodology," *Journal of Biomedical Optics* 24, no. 1 (2019): 1-11.
21. Busca, G., Cigada, A., Mazzoleni, P., and Zappa, E., "Vibration Monitoring of Multiple Bridge Points by Means of a Unique Vision-Based Measuring System," *Experimental Mechanics* 54, no. 2 (2014): 255-271.
22. Patil, K., Baqersad, J., Ludwigsen, D., and Dong, Y., "Extracting Vibration Characteristics of a Guitar Using Finite Element, Modal Analysis, and Digital Image Correlation Techniques," *Proceedings of Meetings on Acoustics* 29, no. 1 (2016): 1-9.
23. Mazzoleni, P. and Zappa, E., "Vision-Based Estimation of Vertical Dynamic Loading Induced by Jumping and Bobbing Crowds on Civil Structures," *Mechanical Systems and Signal Processing* 33 (2012): 1-12.
24. Srivastava, V. and Baqersad, J., "A Multi-View Optical Technique to Extract the Operating Deflection Shapes of a Full Vehicle Using Digital Image Correlation," *Thin-Walled Structures* 145 (2019): 1-9.
25. Atashipour, S. and Baqersad, J., "Mechanical Characterization of Human Skin—A Non-Invasive Digital Twin Approach Using Vibration-Response Integrated with Numerical Methods," *Medical Engineering & Physics* 121 (2023): 1-16.
26. Brons, M., Kasper, T.A., Chauda, G., Klaassen, S.W.B. et al., "Experimental Investigation of Local Dynamics in a Bolted Lap Joint Using Digital Image Correlation," *ASME Journal of Vibration and Acoustics* 142, no. 5 (2020): 051114.
27. Ozbek, M., Rixen, D.J., Erne, O., and Sanow, G., "Feasibility of Monitoring Large Wind Turbines Using Photogrammetry," *Energy* 35, no. 12 (2010): 4802-4811.
28. Lundstrom, T., Baqersad, J., and Niezrecki, C., "Monitoring the Dynamics of a Helicopter Main Rotor With High-Speed Stereophotogrammetry," *Experimental Techniques* 40, no. 3 (2016): 907-919.
29. Mange, A., Baqersad, J., Srivastava, V., and More, J., "Using Digital Image Correlation to Measure Dynamics of Rolling Tires," SAE Technical Paper 2018-01-1217 (2018).
30. Mange, A., Atkinson, T., Bastiaan, J., and Baqersad, J., "An Optical-Based Technique to Obtain Vibration Characteristics of Rotating Tires," *SAE Int. J. Veh. Dyn., Stab., and NVH* 3, no. 3 (2019): 197-208, doi:https://doi.org/10.4271/10-03-03-0013.
31. Swami, A., Liu, C., Kubenz, J., Prokop, G. et al., "Experimental Study on Tire Contact Patch Characteristics for Vehicle Handling with Enhanced Optical Measuring System," *SAE Int. J. Veh. Dyn., Stab., and NVH* 5, no. 3 (2021): 333-350, doi:https://doi.org/10.4271/10-05-03-0023.
32. Zappa, E., Parenzan, L., Montini, E., Melzi, S. et al., "Measurement of the Dynamics of a Tire's Inner Liner With Digital Image Correlation," *IEEE Transactions on Instrumentation and Measurement* 74 (2025): 1-10.
33. Galeazzi, S., Chiariotti, P., Martarelli, M., and Tomasini, E.P., "3D Digital Image Correlation for Vibration

Measurement on Rolling Tire: Procedure Development and Comparison with Laser Doppler Vibrometer," *Journal of Physics: Conference Series* 1149, no. 1 (2018): 1-13.

34. Yeh, Y. and Cummins, H., "Localized Fluid Flow Measurements with an He-Ne Laser Spectrometer," *Applied Physics Letters* 4 (1964): 176-178.
35. Davis, Q.V. and Kulczyk, W.K., "Vibrations of Turbine Blades Measured by Means of a Laser," *Nature* 222, no. 5192 (1969): 475-476.
36. Halliwell, N., "Laser-Doppler Measurement of Vibrating Surfaces: A Portable Instrument," *Journal of Sound and Vibration* 62, no. 2 (1979): 312-315.
37. Bank, G. and Hathaway, G.T., "A Revolutionary 3-D Interferometric Vibrational Mode Display," in *Audio Engineering Society Convention 66, Paper Number 1658*, 1980.
38. Eichenberger, J. and Sauer, J., "Validating Complex Models Accurately and without Contact Using Scanning Laser Doppler Vibrometry (SLDV)," in DiMaio, D. and Baqersad, J., (Eds.), *Rotating Machinery, Optical Methods & Scanning LDV Methods, Volume 6: Proceedings of the 39th IMAC, A Conference and Exposition on Structural Dynamics 2021* (Cham, Switzerland: Springer International Publishing AG, 2021), 113-124.
39. Chiariotti, P., Rembe, C., Castellini, P., Allen, M. et al., "Laser Doppler Vibrometry Measurements in Structural Dynamics," in *Handbook of Experimental Structural Dynamics* (New York: Springer, 2022), 103-147.
40. Nassif, H.H., Gindy, M., and Davis, J., "Comparison of Laser Doppler Vibrometer with Contact Sensors for Monitoring Bridge Deflection and Vibration," *NDT & E International* 38, no. 3 (2005): 213-218.
41. Yang, S. and Allen, M.S., "Output-Only Modal Analysis using Continuous-Scan Laser Doppler Vibrometry and Application to a 20 kW Wind Turbine," *Mechanical Systems and Signal Processing* 31 (2012): 228-245.
42. Riener, T., Goding, A., and Talke, F., "Measurement of Head/Disk Spacing Modulation Using a Two Channel Fiber Optic Laser Doppler Vibrometer," *IEEE Transactions on Magnetics* 24, no. 6 (1988): 2745-2747.
43. Tabatabai, H., Oliver, D.E., Rohrbaugh, J.W., and Papadopoulos, C., "Novel Applications of Laser Doppler Vibration Measurements to Medical Imaging," *Sensing and Imaging* 14, no. 1-2 (2013): 13-28.
44. Mastrodicasa, D., Minervini, D., Lorenzo, E.D., Manzato, S. et al., "Tire Experimental Characterization Using Contactless Measurement Methods," SAE Technical Paper 2021-01-1114 (2021), doi:https://doi.org/10.4271/2021-01-1114.
45. Avitabile, P. and Allemang, R.J., *Handbook of Experimental Structural Dynamics*, 1st ed. (New York: Springer, 2022).
46. Castellini, P. and Montanini, R., "Automotive Components Vibration Measurements by Tracking Laser Doppler Vibrometry: Advances in Signal Processing," *Measurement Science & Technology* 13, no. 8 (2002): 1266-1279.
47. Castellini, P. and Santolini, C., "Vibration Measurements on Blades of a Naval Propeller Rotating in Water with Tracking Laser Vibrometer," *Measurement: Journal of the International Measurement Confederation* 24, no. 1 (1998): 43-54.
48. Gwashavanhu, B., Oberholster, A.J., and Heyns, P.S., "Rotating Blade Vibration Analysis Using Photogrammetry and Tracking Laser Doppler Vibrometry," *Mechanical Systems and Signal Processing* 76-77 (2016): 174-186.
49. Zucca, S., DiMaio, D., and Ewins, D., "Measuring the Performance of Underplatform Dampers for Turbine Blades by Rotating Laser Doppler Vibrometer," *Mechanical Systems and Signal Processing* 32 (2012): 269-281.
50. Brassart, F.P. and Wright, M.E., "A Machine to Study Vertical Tire Stiffness and Damping Coefficient," SAE Technical Paper 932391 (1993), doi:https://doi.org/10.4271/932391.
51. Michelin, "The Tyre: Mechanical and Acoustic Comfort," Société de Technologie Michelin, 2002.
52. Avitabile, P., *Modal Testing: A Practitioner's Guide*, 1st ed. (Hoboken, NJ: Wiley, 2018).
53. Ewins, D.J., *Modal Testing: Theory, Practice and Application*, 2nd ed. (Hoboken, NJ: Wiley, 2009).
54. Blevins, R.D., *Formulas for Natural Frequency and Mode Shape*, Revised & Corrected ed. (Malabar, FL: Krieger Publishing Company, 1995).
55. Bastiaan, J.M. and Khajepour, A., "Finite Element Modeling of Tire with Validation Using Tensile and Frequency Response Testing," in *ASME International Mechanical Engineering Congress and Exposition*, vol. 12, Montreal, QC, Canada, 2014.
56. Choi, W.H. and Bolton, J.S., "FE Simulation of Split in Fundamental Air-Cavity Mode of Loaded Tires: Comparison with Empirical Results," *SAE Int. J. Adv. & Curr. Prac. in Mobility* 4, no. 2 (2022): 419-425, doi:https://doi.org/10.4271/2021-01-1064.
57. Men, X.H. and Zhao, H.Y., "Study on Vibration Characteristics of High-Speed Rotating Constrained Blades Based on Spin Softening," *Applied Mechanics and Materials* 863 (2017): 241-245.

58. Dorfi, H., Wheeler, R., and Keum, B., "Vibration Modes of Radial Tires: Application to Non-Rolling and Rolling Events," SAE Technical Paper 2005-01-2526 (2005), doi:https://doi.org/10.4271/2005-01-2526.
59. Gröhlich, M., Lang, A., Böswald, M., and Meier, J., "Viscoelastic Damping Design—Thermal Impact on a Constrained Layer Damping Treatment," *Materials & Design* 207 (2021): 109885.
60. Higgins, D.D., Marmo, B.A., Jeffree, C.E., Koutsos, V. et al., "Morphology of Ice Wear from Rubber–Ice Friction Tests and its Dependence on Temperature and Sliding Velocity," *Wear* 265, no. 5 (2008): 634-644.
61. Stebbins, M., Poirier, D., Robert, R., and Hornbrook, A., "Dynamic Impact Transient Bump Method Development and Application for Structural Feel Performance," SAE Technical Paper 2020-01-1081 (2020), doi:https://doi.org/10.4271/2020-01-1081.